Journal of Power Sources 196 (2011) 6723–6728

Contents lists available at ScienceDirect

Journal of Power Sources

journal homepage: www.elsevier.com/locate/jpowsour

Performance improvement of polyethylene-supported poly(methyl methacrylate-vinyl acetate)-*co*-poly(ethylene glycol) diacrylate based gel polymer electrolyte by doping nano-Al_2O_3

Y.H. Liao [a], X.P. Li [a,b,c], C.H. Fu [d], R. Xu [d], M.M. Rao [a], L. Zhou [a], S.J. Hu [a,b,c], W.S. Li [a,b,c,*]

[a] *School of Chemistry and Environment, South China Normal University, Guangzhou 510006, China*
[b] *Key Laboratory of Electrochemical Technology on Energy Storage and Power Generation of Guangdong Higher Education Institutes, South China Normal University, Guangzhou 510006, China*
[c] *Engineering Research Center of Materials and Technology for Electrochemical Energy Storage (MOE), South China Normal University, Guangzhou 510006, China*
[d] *Amperex Technology Limited, Dongguan 523080, China*

ARTICLE INFO

Article history:
Received 17 August 2010
Received in revised form 13 October 2010
Accepted 7 November 2010
Available online 13 November 2010

Keywords:
Poly(methyl methacrylate-vinyl acetate)-*co*-poly(ethylene glycol) diacrylate
Nano-aluminum oxide
Gel polymer electrolyte
Electrochemical stability
Lithium ion battery

ABSTRACT

Polyethylene (PE)-supported poly(methyl methacrylate-vinyl acetate)-*co*-poly(ethylene glycol) diacrylate with and without doping nano-Al_2O_3, namely P(MMA-VAc)-*co*-PEGDA/PE and P(MMA-VAc)-*co*-PEGDA/Al_2O_3/PE, are prepared and their performances as gel polymer electrolytes (GPEs) for lithium ion battery are studied by mechanical test, scanning electron microscopy, thermogravimetric analyzer, electrochemical impedance spectroscopy, cyclic voltammetry, and charge/discharge test. It is found that the doping of nano-Al_2O_3 in the P(MMA-VAc)-*co*-PEGDA/PE improves the comprehensive performances of the GPE and thus the rate performance and cyclic stability of the battery. With doping nano-Al_2O_3, the mechanical and thermal stability of the polymer and the ionic conductivity of the corresponding GPE increases slightly, while the battery exhibits better cyclic stability. The mechanical strength and the decomposition temperature of the polymer increase from 15.9 MPa to 16.2 MPa and from 410 °C to 420 °C, respectively. The ionic conductivity of the GPE is from 3.4×10^{-3} S cm^{-1} to 3.8×10^{-3} S cm^{-1}. The discharge capacity of the battery using the GPE with doping nano-Al_2O_3 keeps 90.9% of its initial capacity after 100 cycles and shows good C-rate performance.

1. Introduction

Developing energy storage and conservation technologies is necessary to solve the problems of energy shortage and environmental pollution. Rechargeable lithium ion battery is considered to be an ideal device for energy storage and conservation due to its high energy density. However, there are some issues to be solved for the current commercial lithium ion battery using liquid electrolyte, such as leakage and explosion [1]. Gel polymer electrolyte (GPE), which uses polymer as a matrix to entrap liquid components [2], has been attracting more and more interests because it is safer than liquid electrolyte [3–6]. Many effects have been made to develop new GPEs, but the comprehensive performances (high mechanical strength and high ionic conductivity simultaneously) still need to be improved. The effective way to improve the mechanical strength is to use a mechanical support, such as polyethylene (PE), polypropylene (PP) or non-woven fabrics [7,8], while the drawback of low ionic conductivity can be made up to some extent by copolymerization of monomers or oligomers that have different functions. In our previous work [9], poly(methyl methacrylate-vinyl acetate) (P(MMA-VAc)) was synthesized by emulsion polymerization with methyl methacrylate (MMA) and vinyl acetate (VAc) as monomers. This copolymer combines the advantages with monomer MMA and VAc. MMA provides the copolymer with good electrolyte uptake while VAc provides the GPE with strong adhesion between the anode or/and cathode materials and excellent mechanical stability. However, the highest ionic conductivity of the P(MMA-VAc) based GPE only reaches 1.8×10^{-3} S cm^{-1} and the discharge capacity of the battery using this GPE retains 84.2% of its initial capacity after the 14th cycle at 0.2 C rate. Thus, the performance of P(MMA-VAc) based GPE needs to be further improved.

Co-bridging agent or cross-linker, such as poly(ethylene glycol) dimethacrylate (PEGDMA) and poly(ethylene glycol) diacrylate (PEGDA), has more than two functional groups that can react with other molecules to form a three-dimensional network polymer to absorb the liquid electrolyte effectively. Thus, the performance of a GPE can be reinforced by incorporation with PEGDA or PEGDMA [1,10,11].

* Corresponding author at: School of Chemistry and Environment, South China Normal University, Guangzhou 510006, China. Tel.: +86 20 39310256; fax: +86 20 39310256.
E-mail address: liwsh@scnu.edu.cn (W.S. Li).

0378-7753/$ – see front matter © 2010 Elsevier B.V. All rights reserved.
doi:10.1016/j.jpowsour.2010.11.036

Additionally, the relatively poor performance of GPE can be enhanced to some extent by incorporation of inorganic particles into the polymer matrix [12–15]. Since Croce et al. introduced nano-Al_2O_3 into polyethylene oxide (PEO) system to enhance the low-temperature ion conductivity of the solid polymer electrolyte [16], doping nano-particles in polymers for the performance improvement of GPEs has been paid more and more attentions [15–20]. The nano-Al_2O_3 promotes the ionic conductivity by its high surface area, improves the mechanical strength by its network connected to polymer and enhances the compatibility with electrodes by its interfacial stabilizing action [16].

With the aim to obtain a GPE that has better cyclic stability without the expense of other properties including mechanical strength, ionic conductivity and compatibility with anode and cathode of lithium ion battery, a new copolymer, poly(methyl methacrylate-vinyl acetate)-*co*-poly(ethylene glycol) diacrylate (P(MMA-VAc)-*co*-PEGDA), was synthesized by emulsion polymerization and doped with nano-Al_2O_3, and the performances of this copolymer based GPE were investigated in this paper.

2. Experimental

2.1. Preparation

Commercial monomer MMA (>99.0 wt.%, Fluka), VAc (>99.0 wt.%, Fluka) and oligomer PEGDA (Mw: 400, Aldrich) were mixed in the mass ratio of MMA:VAc:PEGDA = 9:1:1. The synthesis of the P(MMA-VAc)-*co*-PEGDA copolymer was conducted in a four neck glass reactor. 1.5 wt.% sodium dodecyl sulfate (as an emulsifier) solution was prepared with deionized water under N_2 at 60 °C. The mixture (MMA:VAc:PEGDA = 9:1:1 (in mass)) was added into the above solution under stirring vigorously for 1 h to form emulsified solution. After adding initiator and stirring continuously for 6 h, the resulting emulsion was poured into 3 wt.% $Al_2(SO_4)_3$ solution to yield the precipitate, isolated by filtration and washed with hot deionized water (55 °C) in order to remove any impurities such as residual monomers and emulsifier. The P(MMA-VAc)-*co*-PEGDA copolymer in the form of white powder was finally obtained by drying the purified precipitate in a vacuum oven at 55 °C for 12 h and kept in a desiccator for membrane preparation.

The prepared copolymer and nano-Al_2O_3 (Germany Degussa, average particle size of 100 nm) with 10 wt.% content of copolymer were dispersed in acetone at a concentration of 4 wt.% at 40 °C for 2 h. After complete dissolution, a microporous polyethylene (PE) separator (Celgard, USA, thickness: 16 μm) was immersed in the slurry for 1 h, taken out and dried in the air atmosphere for 1 h then in the vacuum at 60 °C for 24 h. P(MMA-VAc)-*co*-PEGDA/Al_2O_3/PE based membrane was obtained.

In order to prepare GPE, the porous membranes were immersed in an electrolyte solution, 1 M $LiPF_6$ in ethylene carbonate (EC)/dimethyl carbonate (DMC)/diethyl carbonate (DEC) (1:1:1 in volume, from Dongguan Shanshan Battery Materials Co., Ltd., battery grade) in an argon-filled glove box (Mikrouna). The GPE without nano-Al_2O_3 was also prepared under the same conditions for comparison.

2.2. Characterization

Mechanical strength measurements were carried out on a Gotech GT-TS-2000 apparatus at a crosshead speed of 50 mm min^{-1}, using standard dumb bell type tensile bars for testing the samples at room temperature. Then the elongation length was measured during the deformation. The morphology of the membranes without and with 10 wt.% nano-Al_2O_3 were characterized by scanning electron microscopy (SEM) (JEOL, JSM-6380LV, Japan) at an acceleration voltage of 15 KV. The thermal stability of the membrane was analyzed with thermogravimetric analyzer (NETZSCH STA 409 PC/PG).

The compatibility of GPE with the anode of lithium ion battery was understood by electrochemical impedance spectroscopy (EIS) using the symmetrical cell Li/GPE/Li with potential amplitude of 5 mV from 500 kHz to 30 mHz. The electrochemical stability of GPE was understood by cyclic voltammetry (CV) with the cell Li/GPE/stainless steel (SS). The SS was used as working electrode and the lithium as the reference and the counter electrodes with the potential scanning rate of 1 mV s^{-1} from −0.5 V to 5 V (vs. Li^+/Li). The CV measurement was conducted with Solartron 1470E (England).

The ionic conductivity of the GPE was determined by the symmetrical cell SS/GPE/SS using EIS with potential amplitude of 5 mV from 500 kHz to 1 Hz. The GPE was sandwiched between two SS discs (diameter Φ = 14 mm). The ionic conductivity was calculated from the bulk electrolyte resistance (R) using the following equation (Eq. (1)):

$$\sigma = \frac{l}{RS} \quad (1)$$

where l is the thickness of the GPE, S is the contact area between GPE and SS disc. The bulk electrolyte resistance was obtained from the complex impedance diagram.

To understand the rate capacity and cyclic stability of lithium ion battery using the developed GPE, a cell Li/GPE/$LiCoO_2$ was set up and charge–discharge test was carried out using Land Battery Test System (Wuhan Land Electronic Co. Ltd.).

3. Results and discussion

3.1. Mechanical strength

Considering the rigorous requirement in the battery manufacture, the mechanical property of a polymer should be considered for its use in GPE [21,22]. Typical stress-deformation curves of PE, P(MMA-VAc)-*co*-PEGDA/PE and P(MMA-VAc)-*co*-PEGDA/Al_2O_3/PE based membranes are shown in Fig. 1. It can be seen from Fig. 1 that the fracture strength of the pure PE membrane, which is widely used in commercial liquid lithium ion battery, is 15.5 MPa. When combining copolymer P(MMA-VAc)-*co*-PEGDA into the PE, similar shape but higher value of the fracture strength (15.9 MPa) can be obtained, as seen in Fig. 1. This suggests that the copolymer can firmly incorporate into the PE membrane. The PEGDA co-bridges with P(MMA-VAc) to form a network structure and helps

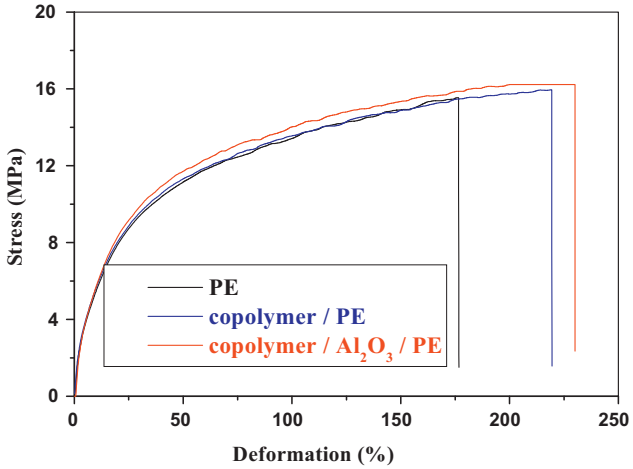

Fig. 1. Engineering stress dependence of engineering deformation of PE, P(MMA-VAc)-*co*-PEGDA (copolymer)/PE and P(MMA-VAc)-*co*-PEGDA (copolymer)/Al_2O_3/PE based membranes.

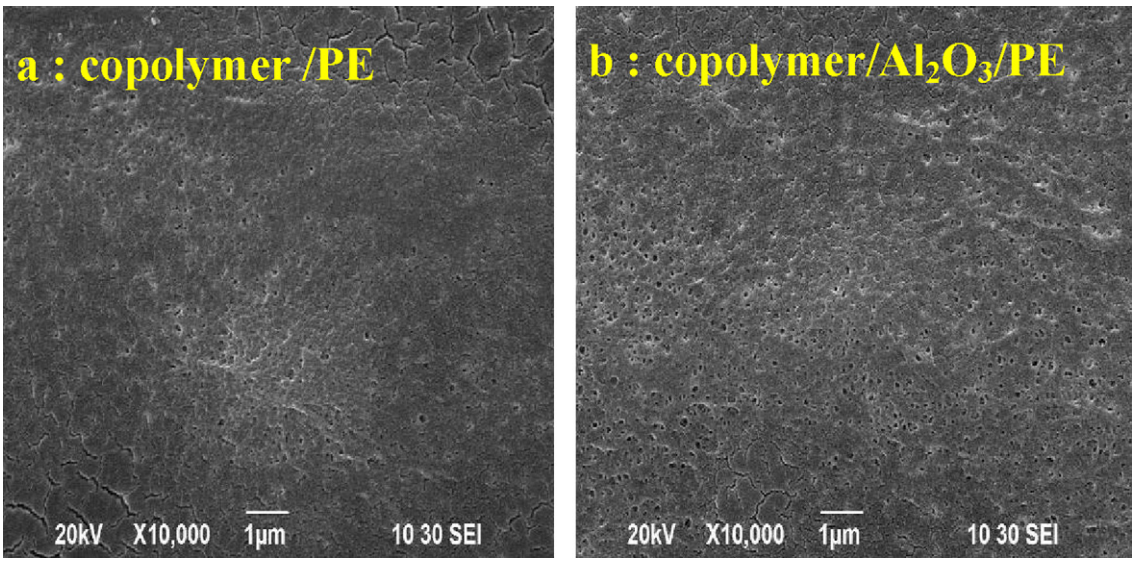

Fig. 2. SEM images of P(MMA-VAc)-*co*-PEGDA (copolymer)/PE and P(MMA-VAc)-*co*-PEGDA (copolymer)/Al_2O_3/PE based membranes.

to increase the mechanical strength. Furthermore, when adding nano-Al_2O_3 into the P(MMA-VAc)-*co*-PEGDA, the fracture strength is increased to 16.2 MPa, indicating that developed membrane possesses good mechanical strength. The reinforcement in mechanical performance should be related to the nano-Al_2O_3 that acts as temporary mechanical connection point and enhances the strength of the membrane.

3.2. Surface morphology

Fig. 2 exhibits SEM images for P(MMA-VAc)-*co*-PEGDA/PE and P(MMA-VAc)-*co*-PEGDA/Al_2O_3/PE membranes. It can be seen from Fig. 2a that the P(MMA-VAc)-*co*-PEGDA copolymer is coated on the PE membrane forming a porous structure, but the pore connectivity is not very well and the pore is sparse in the membrane. The doping of Al_2O_3 in P(MMA-VAc)-*co*-PEGDA improves the pore structure of the membrane, as shown in Fig. 2b. Therefore, it can be expected that the P(MMA-VAc)-*co*-PEGDA/Al_2O_3/PE based GPE has higher ionic conductivity and the battery using this GPE exhibits better rate performance.

3.3. Thermal stability

During the charge and discharge of lithium ion battery, the exothermic reaction takes place. A mass of released heat can make the membrane deformation and even lead to short circuit of the battery. Therefore, the thermal stability of the membrane is essential for a GPE to be used successfully in lithium ion battery [23]. Fig. 3 presents the TGA curves of P(MMA-VAc)-*co*-PEGDA/PE and P(MMA-VAc)-*co*-PEGDA/Al_2O_3/PE based membranes, obtained under N_2 atmosphere from room temperature to 600 °C at a heating rate of 10 °C min^{-1}. The P(MMA-VAc)-*co*-PEGDA/PE based membrane is highly thermal stability, which has no significant mass loss for the temperature up to 410 °C. When adding 10 wt.% nano-Al_2O_3 to the P(MMA-VAc)-*co*-PEGDA/PE, the decomposition temperature of the membrane is improved from 410 °C to 420 °C.

3.4. Compatibility with anode

Interfacial stability between anode and GPE is important for the safety and cyclic stability of lithium ion battery and can be evaluated on the interfacial resistance between lithium and GPE [7]. The interfacial resistance of the cell Li/GPE/Li was surveyed with different storage time at open circuit and Fig. 4 shows the obtained results. It can be found from Fig. 4a that the interfacial resistance of the membrane without nano-Al_2O_3 increases from 160 Ω cm^2 at first day to 225 Ω cm^2 at 25th days. However, the increased magnitude for the membrane with 10 wt.% nano-Al_2O_3 seems much lower. As shown in Fig. 4b, the interfacial resistance of the membrane with nano-Al_2O_3 increases from 152 Ω cm^2 to 203 Ω cm^2 at 25th days. This suggests that doping nano-Al_2O_3 in the polymer improves the compatibility of the GPE with the anode of lithium ion battery. The compatibility improvement can be ascribed to the interfacial stabilizing action of nano-particles [16], which reduce the growth rate of the passive film on anode [24]. Furthermore, the nano-particles with large surface area can effectively hold solvents in the polymer through the capillary force and reduce the reaction activity of the solvents on anode, resulting in a good compatibility of the GPE with the anode [25].

3.5. Electrochemical stability

Fig. 5 presents the voltammograms of P(MMA-VAc)-*co*-PEGDA based GPE without and with 10 wt.% Al_2O_3 using the cell Li/GPE/SS.

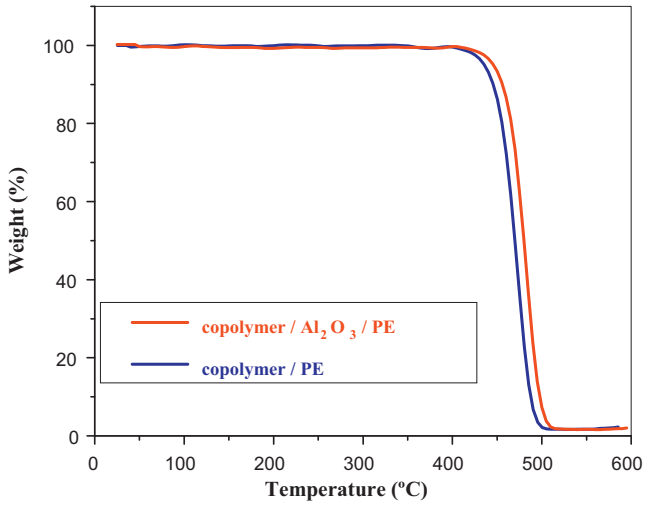

Fig. 3. TG curves of P(MMA-VAc)-*co*-PEGDA (copolymer)/PE and P(MMA-VAc)-*co*-PEGDA (copolymer)/Al_2O_3/PE based membranes.

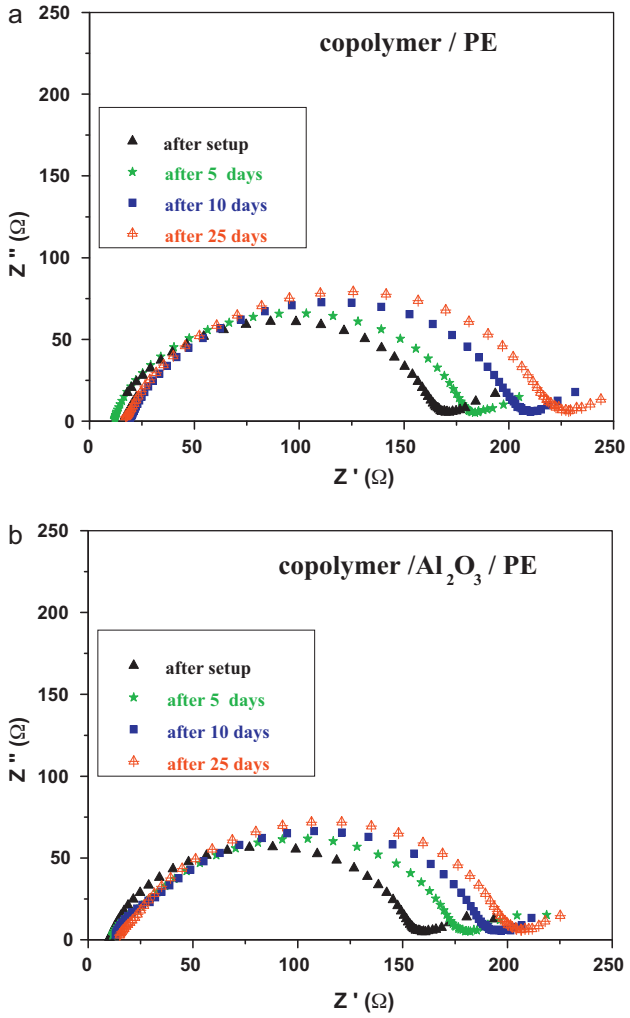

Fig. 4. Nyquist plots of the cell Li/GPE/Li, the GPE based on P(MMA-VAc)-*co*-PEGDA/PE and P(MMA-VAc)-*co*-PEGDA/Al_2O_3/PE.

As seen in Fig. 5, there is no obvious difference between the copolymers without and with Al_2O_3. No reaction takes place in the potential range from 1 V to 5 V except the depositing and stripping of lithium. An anodic peak at about 0.5 V corresponds to the stripping of lithium, while the cathodic peak observed at about −0.46 V should be ascribed to the lithium deposition on the stainless steel electrode. There is no oxidation peak related to the decomposition of GPE in the scanning range, suggesting that the GPE is good enough for the application in the lithium ion battery because the maximum charge voltage for the battery using commercial lithium cobalt oxide as cathode is only 4.2 V.

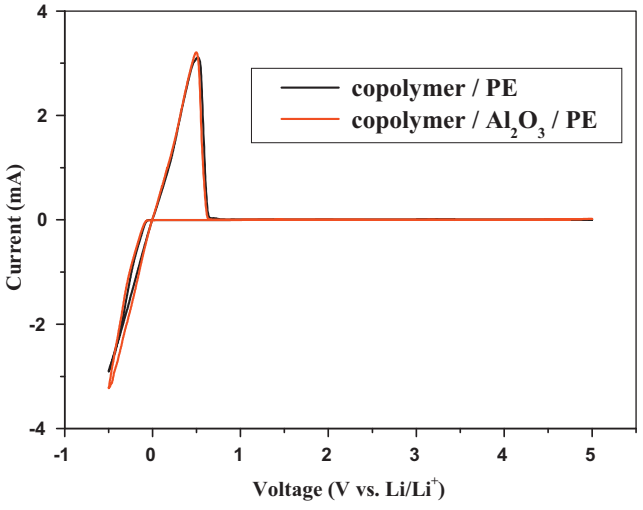

Fig. 5. Cyclic voltammagram of copolymer/PE and copolymer/Al_2O_3/PE based GPEs with the cell structure SS/GPE/Li, scanning rate: 1 mV s^{-1}.

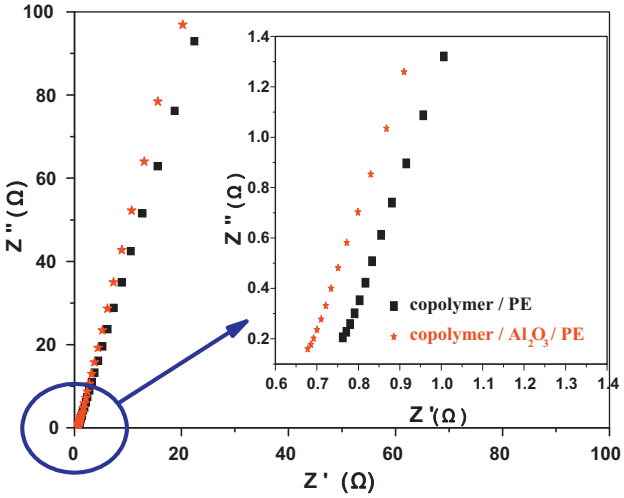

Fig. 6. Nyquist plots of copolymer/PE and copolymer/Al_2O_3/PE based GPEs with the cell structure of SS/GPE/SS at room temperature.

3.6. Ionic conductivity behavior

Fig. 6 presents the Nyquist plots of the cell SS/GPE/SS at room temperature. Based on Eq. (1), the obtained ionic conductivity is 3.8×10^{-3} S cm^{-1} for the GPE with nano-Al_2O_3 and 3.4×10^{-3} S cm^{-1} for the GPE without nano-Al_2O_3, indicating that the doping of nano-Al_2O_3 improves the ionic conductivity of the GPE. These values are much higher than the P(MMA-VAc) based GPE, which is only 1.85×10^{-3} S cm^{-1} [9]. The doping of nanoparticle with large surface area helps to form the membrane with better pore structure (Fig. 2) and thus provides more routes for the ionic transportation, resulting in the enhancement of ionic conductivity.

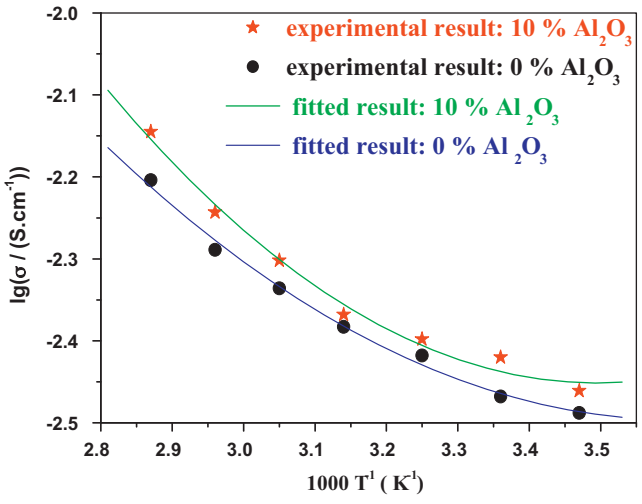

Fig. 7. Temperature dependence of ionic conductivity for copolymer/PE and copolymer/Al_2O_3/PE based GPEs.

Fig. 7 presents the temperature dependence of the ionic conductivity for P(MMA-VAc)-*co*-PEGDA/PE and P(MMA-VAc)-*co*-PEGDA/Al_2O_3/PE based GPEs. The ionic conductivity of the GPEs without and with nano-Al_2O_3 has the same dependence on the temperature. The ionic conductivity increases with the reciprocal temperature, but it is not linear to the reciprocal temperature. This suggests that the doping of nano-Al_2O_3 does not change the conductive mechanism of the GPE, which obeys the Vogel–Tamman–Fulcher (VTF) equation. This behavior is characteristic of the amorphous polymeric electrolyte [26] which follows free-volume model [27,28].

3.7. Battery performance

Fig. 8 shows the discharge curves of the batteries using P(MMA-VAc)-*co*-PEGDA/PE based GPEs without and with nano-Al_2O_3 at different current rates from 4.2 V to 3.0 V. The battery at 0.1 C rate achieves a good capacity, 140 mAh g^{-1} for both the GPEs with and without Al_2O_3. However, when the discharge rate becomes larger, such as 2.0 C, there appears a distinct difference between the batteries using the GPE with and without doping Al_2O_3. The 2.0 C discharge capacity (135 mAh g^{-1}) keeps 96.1% of that at 0.1 C discharge rate for the GPE with nano-Al_2O_3, while the 2.0 C rate discharge capacity (119 mAh g^{-1}) only keeps 86.1% of that at 0.1 C rate for the GPE without Al_2O_3. This indicates that the doping of nano-Al_2O_3 enhances the rate performance of the battery, which can be ascribed to the higher ionic conductivity of the GPE with nano-Al_2O_3 and the lower interfacial resistance between the GPE and electrodes [29].

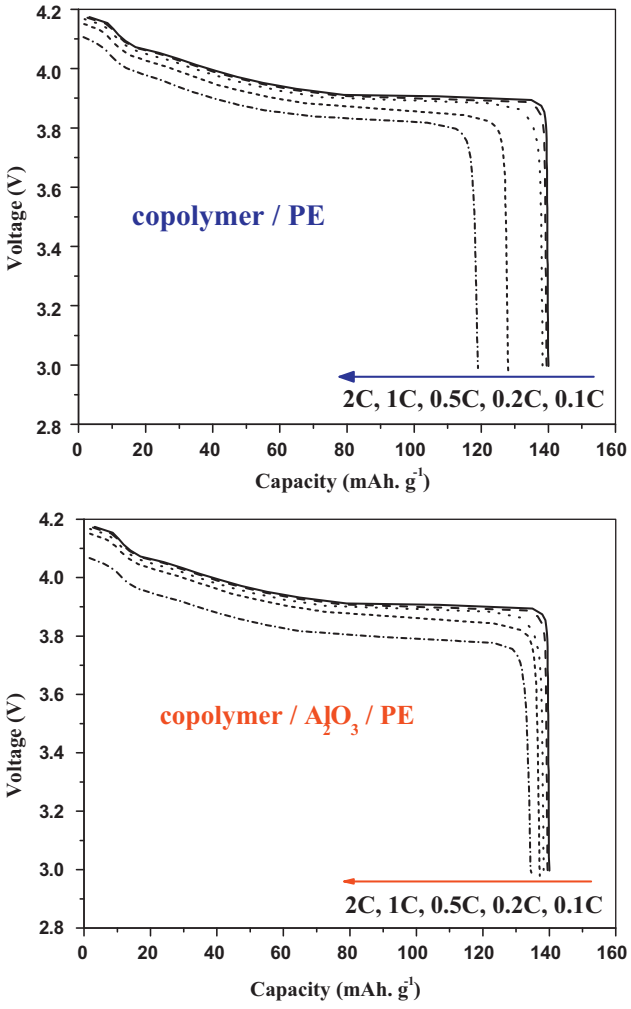

Fig. 8. Rate discharge performance of battery Li/GPE/$LiCoO_2$ at room temperature.

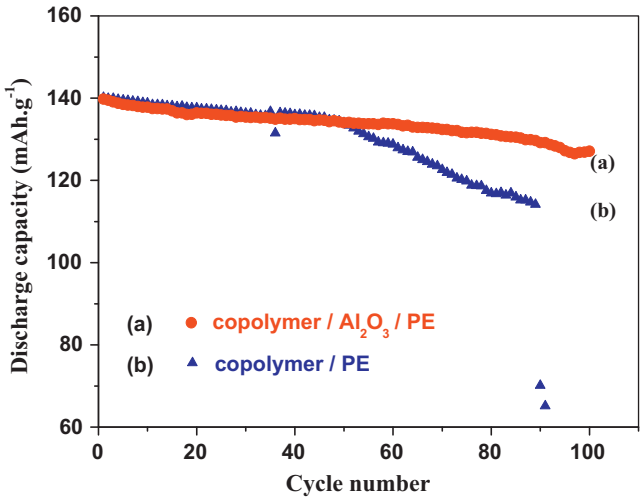

Fig. 9. Cyclic stability of coin cell Li/(copolymer/PE based) GPE/$LiCoO_2$ and Li/(copolymer/Al_2O_3/PE based) GPE/$LiCoO_2$.

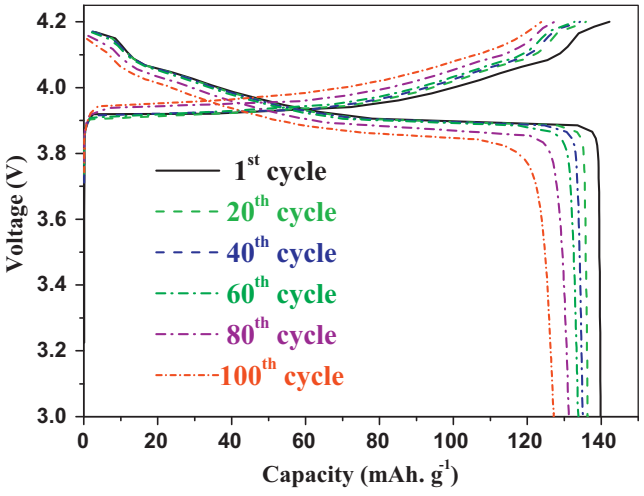

Fig. 10. Charge–discharge curves of the coin cell Li/(copolymer/Al_2O_3/PE based) GPE/$LiCoO_2$ for the 1st, 20th, 40th, 60th, 80th and 100th cycle at the 0.2 C rate between 3.0 V and 4.2 V.

Fig. 9 presents the cyclic stability of the batteries using the GPEs with and without doping nano-Al_2O_3. Both batteries have the same initial capacity and there is no obvious difference in capacity within 50 cycles. However, as the cyclic number increase, discharge capacity of the battery using the GPE without nano-Al_2O_3 is gradually fading, while the battery using the GPE with nano-Al_2O_3 keeps 91% of its initial discharge capacity after the 100th cycle. It is obvious that the doping of nano-Al_2O_3 improves the cyclic stability, which can be ascribed to the better mechanical stability induced by the network of the nano-particles and the better compatibility of the doped GPE with anode. The detailed charge and discharge performance of the battery using the GPE with Al_2O_3 at different cycles is shown in Fig. 10. The charge–discharge plateau is stable, indicating that the developed GPE is good for use in lithium ion battery.

4. Conclusions

A new GPE based on nano-Al_2O_3 doped and PE-supported P(MMA-VAc)-*co*-PEGDA polymer, P(MMA-VAc)-*co*-PEGDA/Al_2O_3/PE, was developed in our lab. With doping nano-Al_2O_3 in the

P(MMA-VAc)-*co*-PEGDA, the mechanical strength and the pore structure of the membrane, the ionic conductivity of the corresponding GPE and its compatibility with anode are improved, thus the battery using this GPE exhibits an enhanced rate performance and cyclic stability.

Acknowledgements

The authors are highly grateful for the financial support from National Natural Science Foundation of China (NNSFC, 20873046), Specialized Research Fund for the Doctoral Program of Higher Education (Grant No. 200805740004) and Natural Science Foundation of Guangdong Province (Grant No. 10351063101000001).

References

[1] F.M. Wang, H.C. Wu, C.S. Cheng, C.L. Huang, C.R. Yang, Electrochim. Acta 54 (2009) 3788–3793.
[2] G.C. Li, Z.H. Li, P. Zhang, H.P. Zhang, Y.P. Wu, Pure Appl. Chem. 80 (2008) 2553–2563.
[3] D.Y. Zhou, G.Z. Wang, W.S. Li, G.L. Li, C.L. Tan, M.M. Rao, Y.H. Liao, J. Power Sources 184 (2008) 477–480.
[4] Y.H. Liao, D.Y. Zhou, M.M. Rao, W.S. Li, Z.P. Cai, Y. Liang, C.L. Tan, J. Power Sources 189 (2009) 139–144.
[5] M.M. Rao, J.S. Liu, W.S. Li, Y. Liang, Y.H. Liao, L.Z. Zhao, J. Power Sources 189 (2009) 711–715.
[6] Y.H. Liao, M.M. Rao, W.S. Li, C.L. Tan, J. Yi, L. Chen, Electrochim. Acta 54 (2009) 6396–6402.
[7] M.M. Rao, J.S. Liu, W.S. Li, Y. Liang, D.Y. Zhou, J. Membr. Sci. 322 (2008) 314–319.
[8] M.K. Song, Y.T. Kim, J.Y. Cho, B.W. Cho, B.N. Popov, H.W. Rhee, J. Power Sources 125 (2004) 10–16.
[9] L. Lu, X.X. Zuo, W.S. Li, J.S. Liu, M.Q. Xu, Acta Chim. Sinica 65 (2007) 475–480.
[10] C.L. Cheng, C.C. Wan, Y.Y. Wang, Electrochem. Commun. 6 (2004) 531–535.
[11] R. Uchiyama, K. Kusagawa, K. Hanai, N. Imanishi, A. Hirano, Y. Takeda, Solid State Ionics 180 (2009) 205–211.
[12] P. Zhang, H.P. Zhang, G.C. Li, Z.H. Li, Y.P. Wu, Electrochem. Commun. 10 (2008) 1052–1055.
[13] J.Y. Xi, X.P. Qiu, L.Q. Chen, Solid State Ionics 177 (2006) 709–713.
[14] S. Ahmad, S.A. Agnihotry, J. Power Sources 140 (2005) 151–156.
[15] Y.H. Liao, M.M. Rao, W.S. Li, L.T. Yang, B.K. Zhu, R. Xu, C.H. Fu, J. Membr. Sci. 352 (2010) 95–99.
[16] F. Croce, G.B. Appetecchi, L. Persi, B. Scrosati, Nature 394 (1998) 456–458.
[17] H.S. Kim, K.S. Kum, W.I. Cho, B.W. Cho, H.W. Rhee, J. Power Sources 124 (2003) 221–224.
[18] Y.J. Wang, D. Kim, Electrochim. Acta 52 (2007) 3181–3189.
[19] M.M. Rao, J.S. Liu, W.S. Li, Y.H. Liao, Y. Liang, L.Z. Zhao, J. Solid State Electrochem. 14 (2009) 255–261.
[20] Z.H. Li, G.Y. Su, X.Y. Wang, D.S. Gao, Chem. J. Chin. U. 24 (2003) 2065–2068.
[21] Z. Tian, X. He, W. Pu, C. Wan, C. Jiang, Electrochim. Acta 52 (2006) 688–693.
[22] C.L. Cheng, C.C. Wan, Y.Y. Wang, M.S. Wu, J. Power Sources 144 (2005) 238–243.
[23] Y.P. Wang, X.H. Gao, R.M. Wang, H.G. Liu, C. Yang, Y.B. Xiong, React. Funct. Polym. 68 (2008) 1170–1177.
[24] Y.X. Jiang, Z.F. Chen, Q.C. Zhuang, J.M. Xu, Q.F. Dong, L. Huang, S.G. Sun, J. Power Sources 160 (2006) 1320–1328.
[25] C.M. Yang, H.S. Kim, B.K. Na, K.S. Kum, B.W. Cho, J. Power Sources 156 (2006) 574–580.
[26] A.M. Christie, L. Christie, C.A. Vincent, J. Power Sources 74 (1998) 77–86.
[27] S. Ahmad, T.K. Saxena, S. Ahmad, S.A. Agnihotry, J. Power Sources 159 (2006) 205–209.
[28] A.M.M. Ali, N.S. Mohamed, A.K. Arof, J. Power Sources 74 (1998) 135–141.
[29] S.S. Zhang, M.H. Ervin, K. Xu, T.R. Jow, Electrochim. Acta 49 (2004) 3339–3345.